

# MACHINE LEARNING-BASED LLRF AND RESONANCE CONTROL OF SUPERCONDUCTING CAVITIES

J. Diaz Cruz\*, S. Biedron<sup>1,2</sup>, S. Sosa

Department of Electrical and Computing Engineering,  
University of New Mexico, Albuquerque, NM 87131, USA

R. Pirayesh, Department of Mechanical Engineering,  
University of New Mexico, Albuquerque, NM 87131, USA

<sup>1</sup>also at Element Aero, Chicago, IL 60643, USA

<sup>2</sup>also at Department of Mechanical Engineering,  
University of New Mexico, Albuquerque, NM 87131, USA

## Abstract

Superconducting radio frequency (SRF) cavities with high loaded quality factors that operate in continuous wave (CW) and low beam loading particle accelerators are sensitive to microphonics induced detuning, which can result in an increase of power to achieve the operational gradient or even in a cavity quench. Such SRF cavities have bandwidths in the order of tens of hertz and detuning requirements can be as tight as 10 Hz. Traditional passive methods to mitigate vibration sources and their impact in the cryomodule/cavity environment have been applied to SRF cavities to reduce microphonics induced detuning. In addition, active resonance control techniques that use stepper motors and piezoelectric actuators to tune the cavity resonance frequency by compensating for microphonics detuning have been investigated. These control techniques could be further improved by applying Machine Learning, which has shown promising results in other control systems of particle accelerators. In this paper, we present an scheme for data production and control parameter optimization, along with a ML framework for LLRF control.

## INTRODUCTION

The quality of X-rays produced in Free Electron Lasers (FEL) depends on the quality of the electron beam. The Low Level RF (LLRF) and resonance control systems are in charge of controlling amplitude and phase of the electromagnetic field inside the superconducting RF (SRF) cavities and the resonance frequency of the SRF cavities. Tight requirements for field control and cavity detuning are common in large facilities like the Linac Coherent Light Source II (LCLS-II), with 0.01% in amplitude, 0.01 degrees in phase and 10 Hz maximum in cavity detuning [1].

Passive techniques to mitigate for microphonics have been applied at Jefferson Lab [2] and Fermilab [3]. Active techniques have also been explored delivering successful results [4,5]. We propose an improvement to these techniques by using Machine Learning (ML), which has been identified as a promising tool that can be used in several subsystems of particle accelerators [6]. For instance, ML has been used

for cavity fault classification at Jefferson Laboratory with an accuracy of 78.2% [7].

In this paper, we propose a ML-based LLRF controller that uses a Neural Network (NN) to calculate the optimal proportional and integral gains to minimize amplitude and phase errors. We also present a data production scheme based on simulations using the CMOC software engine [8] and an algorithm for stochastic optimization [9].

## LLRF MODEL AND DATA PRODUCTION

Traditional LLRF controllers for particle accelerators are PI controllers like the one shown in Fig. 1. It usually consists of a couple of close loops for amplitude and phase. Therefore, the controller has 4 main parameters: proportional and integral gains for amplitude and phase. Tuning this parameters is not a trivial task, specially when the accelerator has an important amount of SRF cavities (280 SRF cavities in the case of the LCLS-II). The tuning process can be optimized to minimize the amplitude and phase stability errors and a NN can be trained to learn this optimization. In the next subsections, we explain the cavity model and the simulations of the close loop.

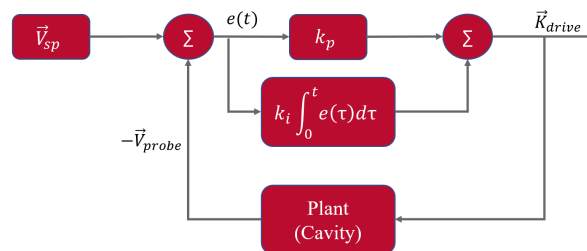


Figure 1: Simplified diagram of a traditional PI LLRF controller.

## Cavity Model

A multi-cell SRF cavity can be modeled as a group of RLC circuits (resonant circuits), each one corresponding to an eigenmode of the cavity. Figure 2 is the equivalent RLC circuit of each eigenmode. The differential equations that describe the electrodynamics of the systems are described

\* jorgedc@unm.edu

in [8] and can be summarized with the following set of equations:

$$V = Se^{j\theta}, \quad (1)$$

$$\frac{d\theta}{dt} = w_d, \quad (2)$$

$$\frac{dS}{dt} = -w_f S + w_f e^{-j\theta} (2K_g \sqrt{R_g} - R_b I), \quad (3)$$

where  $V$  is a representative measure of each mode's energy, with magnitude  $S$  and phase  $\theta$ ,  $w_d$  is the detuning frequency and  $w_f$  is the cavity bandwidth.  $K_g$  is the incident wave amplitude, which represents the power that drives the cavity,  $R_g$  is the coupling impedance of the beam, and  $I$  represents the beam current. This model is used for simulations and data production and allows us to simulate the cavity under the influence of only RF power, or both RF power and electron beam, using different levels of frequency detuning.

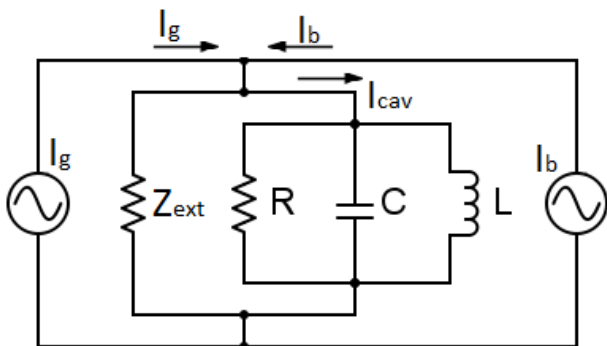


Figure 2: Cavity's circuit model of a resonant mode.

### Closed Loop Simulations

Following the example of the CMOC code [8], we developed our own simplified code to simulate a cavity and a PI controller under the following perturbations: beam loading disturbances, cavity constant detuning and measurement noise. The effects of these perturbations in the stability of the cavity are explained in detail in [10, 11]. In Fig. 3, the top plot shows a cavity (blue curve) reaching the set point (dotted black line) thanks to the action of the control signal  $U$  (red curve). We can see the saturation of the power source for the first 12ms of the simulation, and the effect of 10Hz detuning (oscillating at 200Hz) in the control signal  $U$ . We can also see the effect that beam loading has over the control signal  $U$ , when more power is required when the beam is present (from 15ms to 25ms).

In the bottom plot of Fig. 3, we have a zoom to the cavity's voltage signal to see how it is affected by the perturbations: we see the oscillations due to microphonics, the noise related to the measurement noise, and an undershoot and overshoot related to the start and end of the beam. The upper and lower limits for amplitude stability are shown for reference. The magnitude of the effects related to the perturbations mentioned above is a function of the control parameters

(proportional and integral gains). In the next section we explain how to optimized this parameters to minimize the stability error.

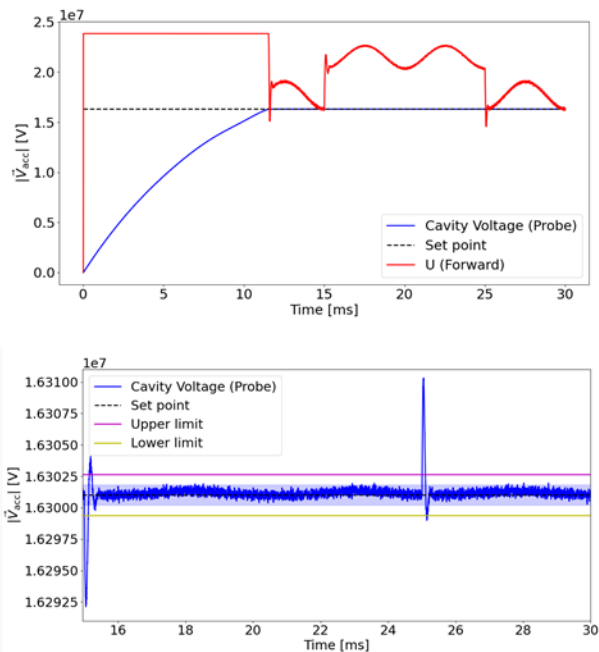


Figure 3: Top: Simulation of the LLRF closed-loop with beam loading disturbances, cavity constant detuning and measurement noise. Bottom: Detail of the cavity's field.

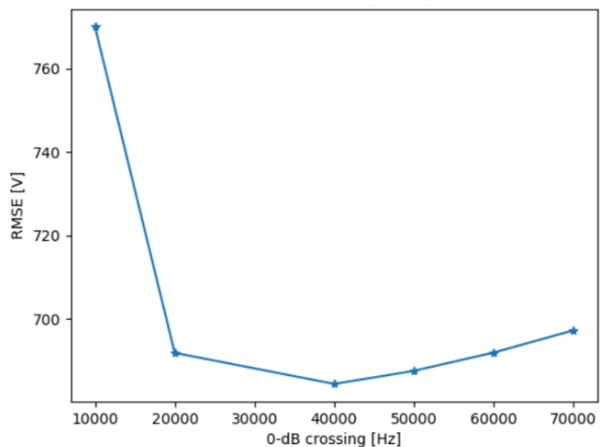


Figure 4: Relation between 0-dB crossing (or proportional gain) and RMSE of cavity's field amplitude.

### CONTROL PARAMETER OPTIMIZATION

The 0-dB crossing of the closed-loop depends on the proportional gain  $k_p$ . Fig. 4 shows the relation between 0-dB crossing (and therefore  $k_p$ ) and the RMSE of the cavity's field amplitude. There is an optimal  $k_p$  that minimizes the error. Applying an algorithm for stochastic optimization using the

python library Noisyopt, described in [9] and represented by the following equation:

$$\min_{k_p} f(k_p) = \min_x E[F(k_p, \xi)], \quad (4)$$

one can find the optimal value of the gain. In Eq. (4),  $f(x)$  represents the RMSE error as a function of the gain, which cannot be directly evaluated, and  $F(x, \xi)$  represents the function that we can simulate and their dependency on a noise  $\xi$ . Using the optimization algorithm and the simulations of the closed-loop, the results of the optimization are shown in Fig. 5. The algorithm can find the optimal gain.

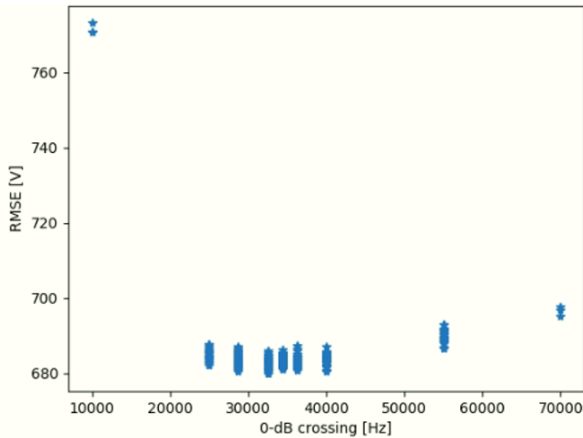


Figure 5: Optimization results.

## ML ARCHITECTURE

A diagram of the ML-based LLRF control system proposed in this paper is shown in Fig. 6. For the optimization and data production phase,  $x_0$  represents the inputs to the optimization algorithm and to the training of the ML.  $x_0$  is the cavity detuning, measurement noise, beam current and set point.  $y$  represents the optimal gain calculated by Noisyopt.  $x_0$  and  $y$  together built the training dataset for the ML. Once the ML is trained, it will be able to calculate the optimal gains,  $\tilde{y}$ , for conditions not seen before,  $\tilde{x}_0$ , and the LLRF controller will use this optimized gains online.

For the optimization and data production phase, and learning phase, we use the resources of the THETA supercomputer at the Argonne Leadership Computer Facility [12]. The experimental phase should be implemented along with the LLRF controller in an FPGA, or in an upper level of software.

## SUMMARY AND FUTURE WORK

Simulations of a closed-loop LLRF system have been implemented based on the CMOC software engine. An algorithm for stochastic optimization called Noisyopt has also been implemented to calculate the optimal proportional gain that minimizes the RMSE of the cavity's field amplitude. An ML-based LLRF controller has been proposed. For the training of the ML, data is produced with the implemented

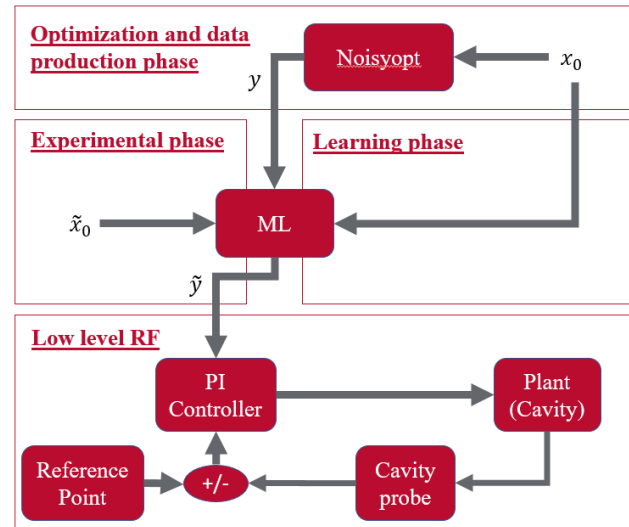


Figure 6: Diagram of the ML-based LLRF control system.

software for simulations and with the Noisyopt algorithm. We plan to develop and deploy the proposed ML-based controller to test it with a cavity emulator.

## ACKNOWLEDGEMENTS

This work is being possible thanks to the guidance of the members of the LCLS-II LLRF team, specially Larry Doolittle, Carlos Serrano and Gang Huang at LBNL, and Andy Benwell and Alex Ratti at SLAC.

This material is based upon work supported by the U.S. Department of Energy, Office of Science, Office of High Energy Physics, under award number DE-SC0019468

This work was performed under Contract No. DE-AC02-76SF00515 supported by the U.S. Department of Energy, Office of Science, Office of Basic Energy Sciences

This research used resources of the Argonne Leadership Computing Facility, which is a DOE Office of Science User Facility. This research also used computing resources of Element Aero

## REFERENCES

- [1] C. Hovater, "Performance and Functional requirements for the LCLS-II Low Level RF System", SLAC, Menlo Park, CA, USA, LCLSII-2.7-FR-0371-R2, Sep. 2017.
- [2] T. Powers, "Control of Microphonics for Narrow Control Bandwidth Cavities", presented at SRF'17, Lanzhou, China, Jun. 2017, unpublished. [https://accelconf.web.cern.ch/srf2017/talks/frxba04\\_talk.pdf](https://accelconf.web.cern.ch/srf2017/talks/frxba04_talk.pdf)
- [3] J. Holzbauer *et al.*, "Passive Microphonics Mitigation during LCLS-II Cryomodule Testing at Fermilab", in *Proc. 9th Int. Particle Accelerator Conf. (IPAC'18)*, Vancouver, Canada, Apr.-May 2018, pp. 2668–2670. doi:10.18429/JACoW-IPAC2018-WEPML001
- [4] N. Banerjee *et al.*, "Active suppression of microphonics detuning in high  $Q_L$  cavities", *Phys. Rev. Accel. Beams*, vol. 22, no. 5, p. 052002, May. 2019. doi:10.1103/PhysRevAccelBeams.22.052002

- [5] J. Holzbauer *et al.*, “Active Microphonics Compensation for LCLS-II”, in *Proc. 9th Int. Particle Accelerator Conf. (IPAC’18)*, Vancouver, Canada, Apr.-May 2018, pp. 2687–2689. doi:10.18429/JACoW-IPAC2018-WEPML007 <https://beamdocs.fnal.gov/AD/DocDB/0049/004978/001/physics.pdf>
- [6] A. Edelen *et al.*, “Opportunities in Machine Learning for Particle Accelerators”, FERMILAB-PUB-19-017-AD, Nov. 2018. arXiv:1811.03172
- [7] C. Tennant *et al.*, “Superconducting radio-frequency cavity fault classification using machine learning at Jefferson Laboratory”, *Phys. Rev. Accel. Beams*, vol. 23, no. 11, p. 114601, Nov. 2020. doi:10.1103/PhysRevAccelBeams.23.114601
- [8] C. Serrano *et al.*, “LCLS-II System Simulations: Physics”, LBNL, Berkeley, CA, USA, Oct. 2015.
- [9] Noisyopt: A Python library for optimizing noisy functions, <https://noisyopt.readthedocs.io/en/latest/index.html>
- [10] J. Diaz Cruz *et al.*, “Studies in Applying Machine Learning to LLRF and Resonance Control in Superconducting RF Cavities”, Oct. 2019. arXiv:1910.07648
- [11] C. Serrano, L. Doolittle and C. Rivetta, “Modeling and Simulations”, LCLS-II LLRF Review, SLAC, Menlo Park, CA, USA, March. 2016.
- [12] Argonne Leadership Computer Facility: Theta, <https://www.alcf.anl.gov/theta>